Traf2 and NCK Interacting Kinase Is a Critical Regulator of Procollagen I Trafficking and Hepatic Fibrogenesis in Mice

Samuel C. Buchl 🄳 ,[1] Zachary Hanquier,[2] Andrew J. Haak,[3] Yvonne M. Thomason,[4] Robert C. Huebert 🄳 ,[1] Vijay H. Shah 🄳 ,[1] and Jessica L. Maiers 🄳 [4]

Hepatic fibrosis is driven by deposition of matrix proteins following liver injury. Hepatic stellate cells (HSCs) drive fibrogenesis, producing matrix proteins, including procollagen I, which matures into collagen I following secretion. Disrupting intracellular procollagen processing and trafficking causes endoplasmic reticulum stress and stress-induced HSC apoptosis and thus is an attractive antifibrotic strategy. We designed an immunofluorescence-based small interfering RNA (siRNA) screen to identify procollagen I trafficking regulators, hypothesizing that these proteins could serve as antifibrotic targets. A targeted siRNA screen was performed using immunofluorescence to detect changes in intracellular procollagen I. Tumor necrosis factor receptor associated factor 2 and noncatalytic region of tyrosine kinase-interacting kinase (TNIK) was identified and interrogated *in vitro* and *in vivo* using the TNIK kinase inhibitor NCB-0846 or RNA interference-mediated knockdown. Our siRNA screen identified nine genes whose knockdown promoted procollagen I retention, including the serine/threonine kinase TNIK. Genetic deletion or pharmacologic inhibition of TNIK through the small molecule inhibitor NCB-0846 disrupted procollagen I trafficking and secretion without impacting procollagen I expression. To investigate the role of TNIK in liver fibrogenesis, we analyzed human and murine livers, finding elevated TNIK expression in human cirrhotic livers and increased TNIK expression and kinase activity in both fibrotic mouse livers and activated primary human HSCs. Finally, we tested whether inhibition of TNIK kinase activity could limit fibrogenesis *in vivo*. Mice receiving NCB-0846 displayed reduced CCl_4-induced fibrogenesis compared to CCl_4 alone, although α-smooth muscle actin levels were unaltered. *Conclusions:* Our siRNA screen effectively identified TNIK as a key kinase involved in procollagen I trafficking *in vitro* and hepatic fibrogenesis *in vivo*. (*Hepatology Communications* 2022;6:593-609).

Hepatic fibrosis develops in response to chronic liver injury, consequently impairing liver function, increasing the risk of carcinogenesis, and leading to liver failure.[1] Fibrogenesis is characterized by deposition of extracellular matrix proteins by nonparenchymal cells, including hepatic stellate cells

(HSCs).[2] HSCs undergo differentiation following liver injury and promote the secretion and deposition of collagen I, the primary component of fibrogenic scar tissue in the liver. While a promising antifibrotic strategy is to target HSCs to limit fibrogenesis or promote resorption of fibrotic matrix, current pharmacologic approaches are ineffective.[3,4] A potentially targetable pathway is intracellular processing and trafficking of the collagen I precursor procollagen I.[3,5] We and others have identified critical chaperones and trafficking proteins involved in procollagen I folding and secretion. Loss or inhibition of these processes limit matrix deposition *in vitro* and fibrogenesis *in vivo*; however, much of the pathway remains unknown, which limits its targetability.[6-8]

Following transcription, procollagen I messenger RNA (mRNA) is cotranslationally translocated into the endoplasmic reticulum (ER). Within the ER, chaperone proteins, including heat shock protein 47 (HSP47), fold and assemble procollagen Iα1 and Iα2 monomers into large heterotrimers that exceed the capacity of canonical coat protein complex II (COPII) ER export vesicles.[8,9] The ER overcomes this limitation through specialized trafficking proteins, including transport and Golgi organization 1 (TANGO1), to facilitate procollagen I ER exit.[7,10,11] Once procollagen I exits the ER, the mechanisms that coordinate and regulate procollagen I trafficking and secretion are unclear. We and others showed that

inhibiting or knocking down proteins involved in procollagen I trafficking, such as TANGO1 or HSP47, alleviates fibrosis in mice.[7,12,13] This occurs through reduced procollagen I secretion as well as apoptosis of activated HSCs. Furthermore, phase 1b/2 clinical trials using liposome-delivered small interfering RNA (siRNA) targeting HSP47 showed promising results limiting fibrosis progression (NCT02227459), highlighting that targeting intracellular procollagen I in HSCs could effectively limit fibrogenesis in patients. Understanding the mechanisms involved in procollagen I trafficking and secretion post-ER could provide key insights into antifibrotic strategies.

Here, we endeavored to identify proteins involved in procollagen I trafficking in HSCs that could be targeted *in vivo* to limit fibrogenesis. To this end, we performed a targeted siRNA screen to identify genes involved in procollagen I secretion. Out of 144 genes involved in membrane trafficking, knockdown of nine genes significantly increased intracellular procollagen I retention, of which seven had no previously known role in procollagen I trafficking. One of the top targets was tumor necrosis factor receptor associated factor 2 and noncatalytic region of tyrosine kinase-interacting kinase (TNIK), a serine/threonine kinase. We investigated the role of TNIK *in vitro* and found that deletion or pharmacologic inhibition of TNIK kinase activity disrupted procollagen I trafficking and secretion without reducing procollagen I expression.

ARTICLE INFORMATION:

From the [1]Division of Gastroenterology and Hepatology, Mayo Clinic, Rochester, MN, USA; [2]Department of Medical and Molecular Genetics, Indiana University School of Medicine, Indianapolis, IN, USA; [3]Department of Physiology and Biomedical Engineering, Mayo Clinic, Rochester, MN, USA; [4]Division of Gastroenterology, Indiana University School of Medicine, Indianapolis, IN, USA.

ADDRESS CORRESPONDENCE AND REPRINT REQUESTS TO:

Jessica L. Maiers, Ph.D.
Division of Gastroenterology
Indiana University School of Medicine
702 Rotary Circle
Indianapolis, IN 46202, USA
E-mail: jemaiers@iu.edu
Tel.: +1-317-274-8157

Furthermore, TNIK kinase activity and expression increased in both human and murine models of liver fibrosis. Finally, pharmacologic inhibition of TNIK kinase activity limited CCl_4-induced hepatic fibrogenesis *in vivo*. Together, this work identifies TNIK as a critical and targetable component of the procollagen I trafficking pathway in HSCs and establishes a new platform for identifying candidate antifibrotic targets to disrupt procollagen intracellular processing and trafficking.

Materials and Methods

siRNA IMMUNOFLUORESCENCE SCREEN

We individually reverse transfected into LX-2 cells 144 siRNA constructs (Dharmacon Human ON-TARGETplus siRNA Library-Membrane Trafficking; set of 4, 0.1 nmol) and an siRNA targeting TANGO1 (positive control). 48 hours after transfection, cells were treated with 5 ng/mL transforming growth factor β1 (TGFβ1) for 24 hours, fixed in 4% paraformaldehyde, permeabilized in 0.1% Triton X-100, and blocked in 3% bovine serum albumin (BSA) in phosphate-buffered saline (PBS). Cells were stained with an antibody targeting procollagen I (Supporting Table S1) as well as with CellMask and 4′,6-diamidino-2-phenylindole (DAPI) to stain the cell membrane and nucleus, respectively. A Cytation 5 multiplate reader was used to image and measure intracellular procollagen levels. Procollagen I immunofluorescence was measured using the following three separate analyses: 1) mean object fluorescence (average green fluorescence/cell); 2) confluence (percentage of cell area with green fluorescence); and 3) total intensity (total fluorescence/cell number). Genes whose knockdown increased procollagen I retention compared to the siControl in all analyses ($P < 0.1$) in three biological replicates were selected for further analysis.

CELL CULTURE

Immortalized human HSCs (hHSCs) (LX-2; ATCC) or primary hHSCs (ScienCell) were cultured in Dulbecco's modified Eagle's medium (DMEM; Gibco) with 10% fetal bovine serum (FBS; Atlanta Biological) and 1% penicillin/streptomycin (Gibco). For all experiments using compounds in conjunction with TGFβ, cells were serum starved in basal DMEM 4 hours before TGFβ treatment (2 ng/μL for hHSCs, 5 ng/μL for LX-2 cells) in vehicle (4 mM Hydrogen chloride [HCl] in 0.1% BSA in double-distilled water [ddH_2O]) or vehicle alone in basal DMEM. For *in vitro* experiments using NCB-0846, we added NCB-0846 (0.1 μM in dimethyl sulfoxide [DMSO]) or DMSO alone to the cells concurrently with TGFβ. MC3T3-E1 cells were a generous gift from Dr. Joseph Bidwell and were cultured in α-minimal essential medium (Life Technologies) with 10% FBS, 1% penicillin/streptomycin (Corning), and 1% L-glutamine (Hyclone).

MICE

Mice were treated in accordance with protocols approved by the Institutional Animal Care and Use Committee of Mayo Clinic. Mice were housed in transparent polycarbonate cages subjected to 12-hour light/dark cycles at 21°C and 50% relative humidity. All interventions were performed during the light cycle. A standard chow diet and fresh water were provided *ad libitum*. Fibrosis was induced in age- and sex-matched c57Bl/6J mice through twice weekly intraperitoneal injections of CCl_4 (0.5 μL/mg, 0.08 mL/mouse) or olive oil. The TNIK kinase inhibitor NCB-0846 (BOC Sciences) was resuspended in 70% polyethylene glycol 300, 15% DMSO, and 15% ddH_2O (0.3 mg in 30 μL of vehicle). NCB-0846 or vehicle alone was administered by intraperitoneal injection 5 times per week on non-CCl_4 injection days at a dose of 10 mg/kg (n = 6-9 mice/group). After 28 days, mice were sacrificed and livers prepared for assessment by sirius red, immunoblotting, quantitative polymerase chain reaction (qPCR), and hydroxyproline assays. Sirius red staining was performed by the Mayo Clinic Biomaterials and Histomorphometry Core Facility. Four images were taken per tissue (magnification ×5) and analyzed using ImageJ. Hydroxyproline analysis was performed by digesting tissue in 6 N HCl overnight at 95°C, followed by dehydration using a vacuum concentrator, resuspension in water, and filtration using 0.22-μm filter centrifuge tubes (Corning). Samples were mixed with chloramine-T (1.41 g in 10 mL ddH_2O, 10 mL n-propanol, and 80 mL acid buffer [12.5 g citric acid monohydrate, 3 mL glacial acetic acid, 30 g sodium

acetate trihydrate, 8.5 g NaCl, brought up to 250 mL, and added to 50 mL ddH$_2$O and 75 mL n-propanol], pH 6.0). Samples were mixed with Ehrlich-perchloric acid (1.5 g p-dimethylaminobenzaldehyde in 6 mL n-propanol, 2.22 mL 60% perchloric acid, and 1.78 mL ddH$_2$O). Samples were heated at 65°C for 15 minutes, moved to room temperature for 20 minutes, and read at 561 nm using a spectrophotometer.

TRANSIENT TRANSFECTIONS

LX-2 cells were transfected with siRNA (GE Dharmacon) to inhibit gene expression. siRNA was delivered by Oligofectamine (Invitrogen) or RNA interference (RNAi)Max (Invitrogen) per the manufacturers' protocols.

GENERATION OF STABLE CELL LINES

LentiCas9-Blast was a gift from Dr. Feng Zhang (Addgene #52962); viral packaging plasmids pMD2.G and psPAX2 were gifts from Dr. Didier Trono (Addgene #12260 and #12259); and the TNIK guide RNA (gRNA) for clustered regularly interspaced short palindromic repeats (CRISPR)-mediated knockout was a gift from Dr. John Doench and Dr. David Root (Addgene #75851).[14,15] To stably knock out TNIK, HEK293T cells were transfected with LentiCas9-Blast and the TNIK gRNA along with viral packaging plasmids psPAX2 and pMD2.G, using Lipofectamine 3000 (Invitrogen). At 36 hours and 60 hours after transfection, virus-containing supernatant from HEK293T cells was harvested, filtered, and used to infect LX-2 cells. Selection was performed using blasticidin (10 μg/mL) and puromycin (2 μg/mL). To generate cells that stably express membrane-bound green fluorescent protein (mGFP)–collagen type I alpha 1 (Col1α1), pLVX-streptavidin-binding protein (SBP)-mGFP-Col1α1 (Addgene #110726) was transfected into HEK293T cells along with viral packaging plasmids P8.91 and VSV-G, using Effectene (Qiagen). Viral particles were harvested and used to infect LX-2 cells. Infected cells were selected using puromycin (2 μg/mL).

IMMUNOBLOTTING

Conditioned media was harvested from cells, centrifuged to remove cell debris, and concentrated using Amicon Ultra Centrifuge filters (Millipore Sigma). Cells were rinsed with PBS and lysed in radio immunoprecipitation assay buffer (Fisher Scientific) plus Halt Protease Inhibitor (ThermoFisher). Lysates were homogenized, centrifuged to remove cell debris, denatured in 6× Lamelli buffer plus β-mercaptoethanol, and resolved by sodium dodecyl sulfate–polyacrylamide gel electrophoresis. The bottom portion of conditioned media gels was removed for Coomassie staining, which served as a loading control. Proteins were transferred onto nitrocellulose, blocked, and incubated overnight in primary antibodies. Appropriate horseradish peroxidase (HRP)-conjugated secondary antibodies were added, and blots were developed using chemiluminescence. For analysis of liver tissues, whole liver was processed as described.[7] Antibodies are listed in Supporting Table S1. All experiments were performed with a minimum of three biological replicates, and quantification and statistical analysis were performed using ImageJ and GraphPad Prism, respectively.

IMMUNOFLUORESCENCE

Treated hHSCs were fixed in 4% paraformaldehyde, permeabilized in 0.1% Triton X-100, and blocked in 3% BSA in PBS. For experiments measuring extracellular collagen I, permeabilization was omitted. hHSCs were stained with primary antibodies (Supporting Table S1) and costained with DAPI to label the nucleus. Images were taken using an AxioObserver Z1 Live Cell microscope with Definite Focus. Six to eight images were taken per condition and analyzed by ImageJ.

IMMUNOHISTOCHEMISTRY

Immunohistochemistry (IHC) was performed as described.[16] In brief, paraffin-embedded tissues were deparaffinized, rehydrated, and stained with an antibody targeting α-smooth muscle actin (αSMA) (Table S1). Five images were taken per mouse (magnification ×10) and analyzed by ImageJ.

SIRCOL ASSAY

To promote mineralization of MC3T3-E1 cells, media was supplemented with 50 μg/mL ascorbic acid and 5 mM beta-glycerophosphate. DMSO or

0.2 μM NCB-0846 was added at the time of mineralization. At 24 hours following treatment, total collagen I levels were analyzed using Sircol Soluble Collagen Assay (Biocolor) following the manufacturer's protocol.[17]

qPCR ANALYSIS

Cells or tissues were lysed in TRIzol (Invitrogen), and mRNA was harvested using the RNeasy Mini Kit (Qiagen) per the manufacturer's instructions. Equal amounts of mRNA were reversed transcribed to complementary DNA and analyzed by qPCR. Primer sequences are listed in Supporting Table S2.

PROCOLLAGEN I TRAFFICKING TEMPERATURE–PULSE ASSAY

mGFP-Col1α1 cells were ascorbate starved overnight, treated with NCB-0846 (0.1 μM) or DMSO, and shifted to 40°C for 3 hours to prevent procollagen I folding and exit from the ER.[18,19] After 3 hours, cells were either fixed immediately (0 minutes) or treated with ascorbate and shifted to 32°C for 60 minutes to permit procollagen I folding and secretion from the ER. Cells were fixed, permeabilized, and stained with DAPI to label nuclei. Images were taken using an AxioObserver Z1 Live Cell microscope with Definite Focus (eight images per condition per replicate) and analyzed using ImageJ software.
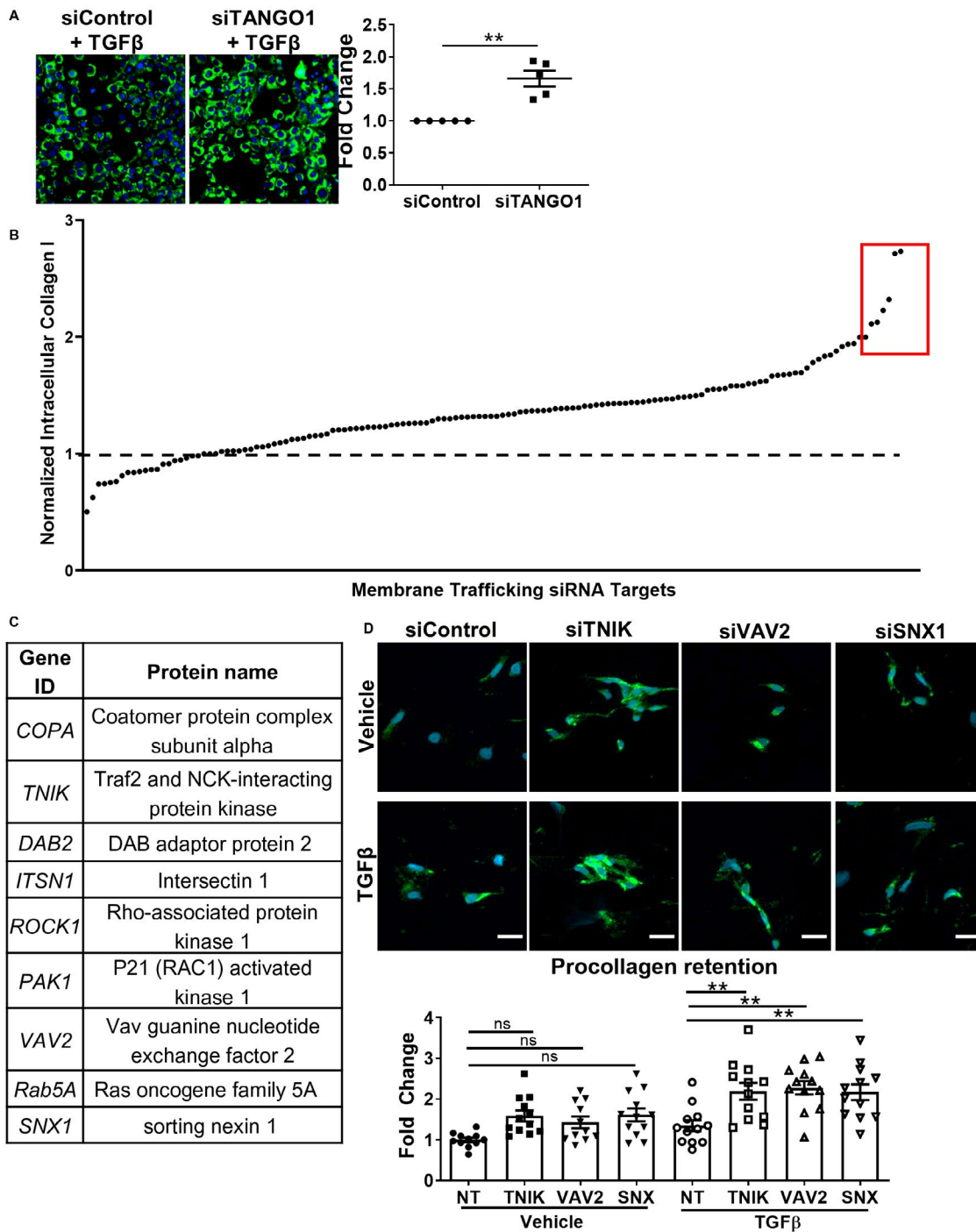
CELL DEATH DETECTION

In vitro terminal deoxynucleotidyl transferase–mediated deoxyuridine triphosphate nick-end labeling (TUNEL) staining was performed with the *In Situ* Cell Death Detection Kit, Fluorescein (Roche). Cells were treated with TGFβ (or vehicle) with or without NCB-0846 (0.1 μM) or DMSO for 48 hours, fixed with 4% paraformaldehyde, and costained for TUNEL (following the manufacturer's protocol) and DAPI. Cells were imaged using an AxioObserver Z1 Live Cell microscope with Definite Focus (eight images per condition per replicate) and analyzed using ImageJ software. For *in vivo* analysis of cell death, paraffin-embedded liver tissues were processed and stained for TUNEL staining by the Histology Services Core at the Indiana University School of Medicine using the TUNEL Chromogenic Apoptosis

Detection Kit (ABP Biosciences). In brief, slides were deparaffinized, rehydrated, and placed in 0.01 M citrate buffer at 37°C. Following peroxidase quenching, terminal transferase reaction buffer was added to the slides overnight. The following day, slides were rinsed with PBS, stained with HRP-streptavidin, and developed with 3,3′-diaminobenzidine. A 0.2% methyl green solution was used as a counterstain. Five images per slide were taken (magnification ×10) and analyzed using ImageJ.

Results

IDENTIFICATION OF TNIK AS A KEY PROCOLLAGEN I TRAFFICKING PROTEIN

To identify novel players in procollagen I trafficking, we established a screening platform to efficiently and accurately measure procollagen I retention by immunofluorescence. LX-2 cells were plated in a 96-well glass-bottom plate and transfected with siRNA targeting TANGO1 or a scrambled control. Transfected cells were treated with TGFβ, fixed, permeabilized, and incubated in a primary antibody against procollagen I. The cells were imaged and quantified, validating that TANGO1 loss increases intracellular procollagen I retention (green; Fig. 1A). Integrated density between siControl and siTANGO1 cells treated with TGFβ was compared to ensure that a measurable increase in procollagen I retention could be observed following TANGO1 loss, as described.[7] We used this platform to screen 144 genes involved in membrane trafficking (Dharmacon). LX-2 cells were reverse transfected with individual siRNAs, treated with TGFβ for 24 hours, and stained for procollagen I. DAPI was used to analyze cell number, and CellMask stain labeled the plasma membrane to confirm intracellular procollagen I localization (Fig. 1B). Nine genes showed robust intracellular procollagen I retention across three biological replicates (Fig. 1C). Two identified genes, coatamer subunit alpha (COPA) and rho-associated protein kinase 1 (ROCK1), have previously been implicated in procollagen I trafficking or regulation, so further experimentation focused on the remaining seven targets.[20-22] We confirmed these targets by transfecting LX-2 cells with an siRNA against each target

A siControl + TGFβ / siTANGO1 + TGFβ

B

C

Gene ID	Protein name
COPA	Coatomer protein complex subunit alpha
TNIK	Traf2 and NCK-interacting protein kinase
DAB2	DAB adaptor protein 2
ITSN1	Intersectin 1
ROCK1	Rho-associated protein kinase 1
PAK1	P21 (RAC1) activated kinase 1
VAV2	Vav guanine nucleotide exchange factor 2
Rab5A	Ras oncogene family 5A
SNX1	sorting nexin 1

D siControl / siTNIK / siVAV2 / siSNX1

Procollagen retention

or a control siRNA, followed by TGFβ treatment. Immunofluorescence was performed to compare the response to TGFβ and/or a vehicle control. TNIK, vav guanine nucleotide exchange factor 2 (VAV2), and syntaxin 1 (SNX1) were the top three genes that, when knocked down, resulted in procollagen I retention following TGFβ treatment (Fig. 1D).

TNIK KNOCKDOWN AND KNOCKOUT DISRUPT PROCOLLAGEN I SECRETION

The robust increase of procollagen I retention in response to TNIK loss led us to further investigate the role of TNIK in procollagen I secretion.

FIG. 1. Genetic screening identified TNIK as a putative procollagen trafficking protein. (A) LX-2 cells (immortalized HSCs) were plated and transfected with siRNA against TANGO1 or a nontargeting control. Cells were serum starved and treated with TGFβ (5 ng/mL) for 24 hours, followed by staining with an antibody targeting procollagen I (green) or DAPI (nucleus, blue) to confirm the efficacy of the screening platform. Images were taken at magnification ×10 with six images taken per well and analyzed using a Cytation 5 Cell Imaging Multi-Mode Reader (n = 5). (B) LX-2 cells were reverse transfected with one of 144 siRNAs or a nontargeted control followed by serum starvation and TGFβ treatment (5 ng/mL) for 24 hours. Cells were fixed and stained with a procollagen I antibody (green), CellMask (red), and DAPI (blue) to allow for quantification of intracellular procollagen. Images were taken at magnification ×10 and analyzed using a Cytation 5 Cell Imaging Multi-Mode Reader with six images taken per well. Procollagen I retention was calculated as the integrated density of procollagen I per cell, normalized to siControl, and presented in graphic format (n = 3). (C) Nine genes led to increased procollagen I retention ($P < 0.1$). (D) To confirm top hits, LX-2 cells were transfected with siRNA targeting *TNIK*, *VAV2*, *SNX1*, or a nontargeting control, followed by treatment with TGFβ or a vehicle control for 24 hours. Cells were fixed, permeabilized, and stained with an antibody targeting procollagen I (green) or DAPI (blue). Images were taken at magnification ×10 using an AxioObserver 5 microscope (scale bar, 50 μm; n = 12). **$P < 0.01$, as determined by a paired Student t test for panel A or one-way ANOVA followed by Tukey post hoc analysis for panel D. Bars in panels A and D represent mean ± SEM. Abbreviations: ns, not significant; NT, nontargeting control; SNX1, Syntaxin 1; VAV2, vav guanine nucleotide exchange factor 2.

siTNIK cells were treated with TGFβ or vehicle, after which cell lysates and conditioned media were harvested. TNIK knockdown disrupted secretion of procollagen I as well as fibronectin, another matrix protein produced by activated HSCs (Fig. 2A), without impacting intracellular procollagen I protein levels (Fig. 2B). To confirm the effects of TNIK loss on matrix secretion, we used CRISPR-Cas9 to stably knock out TNIK expression from LX-2 cells (gTNIK) (Fig. 2C). Cas9-mediated deletion of TNIK effectively reduced secretion of collagen I, although the effect on fibronectin secretion was modest (Fig. 2D). Further analysis revealed that TNIK loss also impacted secretion of another collagen isoform, collagen III (Supporting Fig. S1). Together, these data confirm that TNIK is critical for procollagen I/III secretion from HSCs as well as impacts fibronectin secretion.

TNIK KINASE ACTIVITY IS REQUIRED FOR PROCOLLAGEN SECRETION

TNIK is a serine/threonine kinase encoding 1,360 amino acids with an N-terminal kinase domain, a central domain, and a C-terminal citron homology domain.[23] Its kinase activity is involved in cytoskeletal remodeling, endosomal trafficking, and Wnt signaling.[23-26] TNIK also undergoes autophosphorylation at S764 following binding to proteins, including member of RAS oncogene family Rap2A, and this autophosphorylation serves as a readout of its activity.[26,27] To determine if TNIK kinase activity is critical for trafficking and secretion of procollagen I and fibronectin, we took advantage of a small molecule

inhibitor of TNIK kinase activity, NCB-0846.[28] Primary hHSCs were treated with NCB-0846 (0.1 μM) followed by TGFβ treatment (2 ng/mL, 24 hours). NCB-0846 limited TNIK autophosphorylation at S764 in response to TGFβ (Fig. 3A). NCB-0846 treatment also limited secretion of collagen I and fibronectin (Fig. 3B). Importantly, NCB-0846 treatment did not impact TGFβ-induced procollagen I transcription, further highlighting that TNIK regulates procollagen posttranscriptionally (Fig. 3C). We also analyzed procollagen/collagen I levels either intracellularly or extracellularly using immunofluorescence, observing that NCB-0846 increased procollagen I retention (Fig. 3D) while limiting deposited collagen I (Fig. 3E).

To validate the role of TNIK in modulating procollagen trafficking in a system without TGFβ, we used a temperature-pulsing protocol.[19] LX-2 cells were engineered to stably express pLVX-SBP-mGFP-Col1α1, which is a GFP-tagged procollagen Iα1 construct that traffics normally but the GFP-tag is cleaved following secretion.[18] mGFP-Col1α1-expressing cells were treated with DMSO or NCB-0846 and incubated at 40°C for 3 hours to prevent procollagen exit from the ER. Cells were then shifted to 32°C to allow procollagen 1α1 exit from the ER and trafficking through the secretory pathway. At 60 minutes following the shift to 32°C, cells were fixed and analyzed by microscopy. Vehicle-treated cells showed a 51% decrease in intracellular mGFP-Col1α1 after 60 minutes; however, cells treated with NCB-0846 only showed a 14% decrease in intracellular mGFP-Col1α1 (Fig. 3F). These data indicate that procollagen I trafficking is delayed in the presence of NCB-0846.
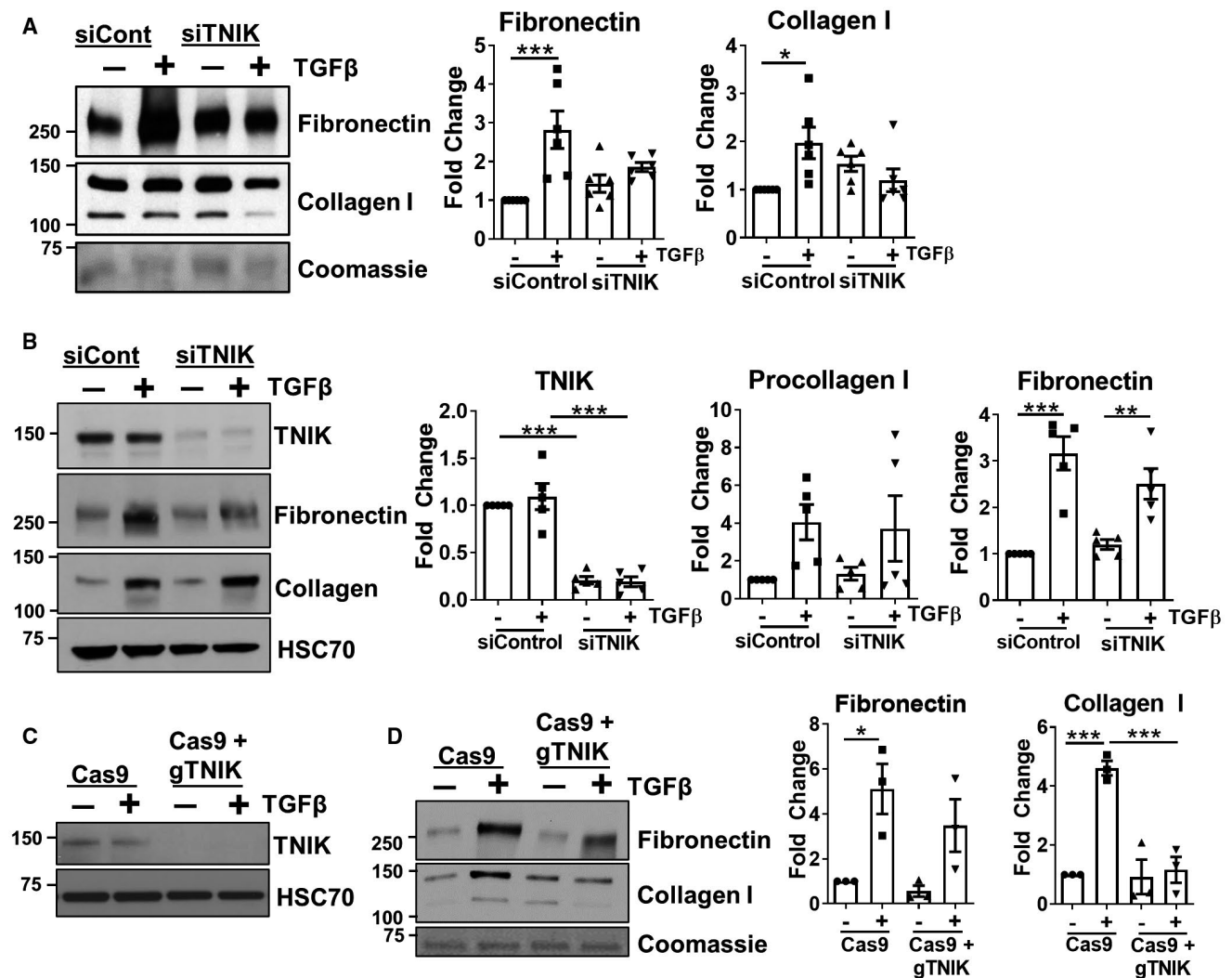
FIG. 2. TNIK knockdown disrupts procollagen I secretion. LX-2 cells were transfected with an siRNA targeting TNIK and followed by TGFβ treatment (5 ng/mL, 24 hours). (A) Conditioned media or (B) cell lysates were harvested and analyzed by immunoblotting for extracellular or intracellular proteins, respectively (n = 4 for conditioned media analysis and n = 5 for cell lysate analysis). (C,D) LX-2 cells stably expressing Cas9 alone or Cas9 plus a guide RNA targeting TNIK were treated with vehicle or TGFβ (5 ng/mL, 24 hours). (C) Whole-cell lysates or (D) conditioned media were harvested and analyzed for protein levels of (C) TNIK or (D) fibronectin and collagen I with HSC70 or Coomassie staining as loading controls (n = 3). *P < 0.05, **P < 0.01, ***P < 0.001, as calculated by one-way ANOVA followed by Tukey post hoc test. Bars in panels A–D represent mean ± SEM. Abbreviation: gTNIK, guide RNA targeting TNIK.

We next sought to determine whether the role of TNIK in procollagen I trafficking is conserved between HSCs and procollagen I–producing osteoblasts. We induced mineralization of MC3T3-E1 osteoblasts in the presence of NCB-0846 (0.2 μM) or vehicle, and analyzed extracellular collagen levels using a Sircol assay. Intriguingly, NCB-0846 treatment did not limit collagen deposition despite inhibiting TNIK phosphorylation (Supporting Fig. S2B,C).

Due to the clear role of TNIK in procollagen I trafficking in HSCs, we investigated whether TNIK inhibition led to procollagen I retention in two major secretory organelles, the ER and the Golgi. Interestingly, procollagen I did not colocalize with either the ER-marker calnexin or the trans-Golgi-marker p230 trans-Golgi following NCB-0846 treatment (Supporting Fig. S3A,B), indicative of a potential role for TNIK in post-Golgi vesicle trafficking. We
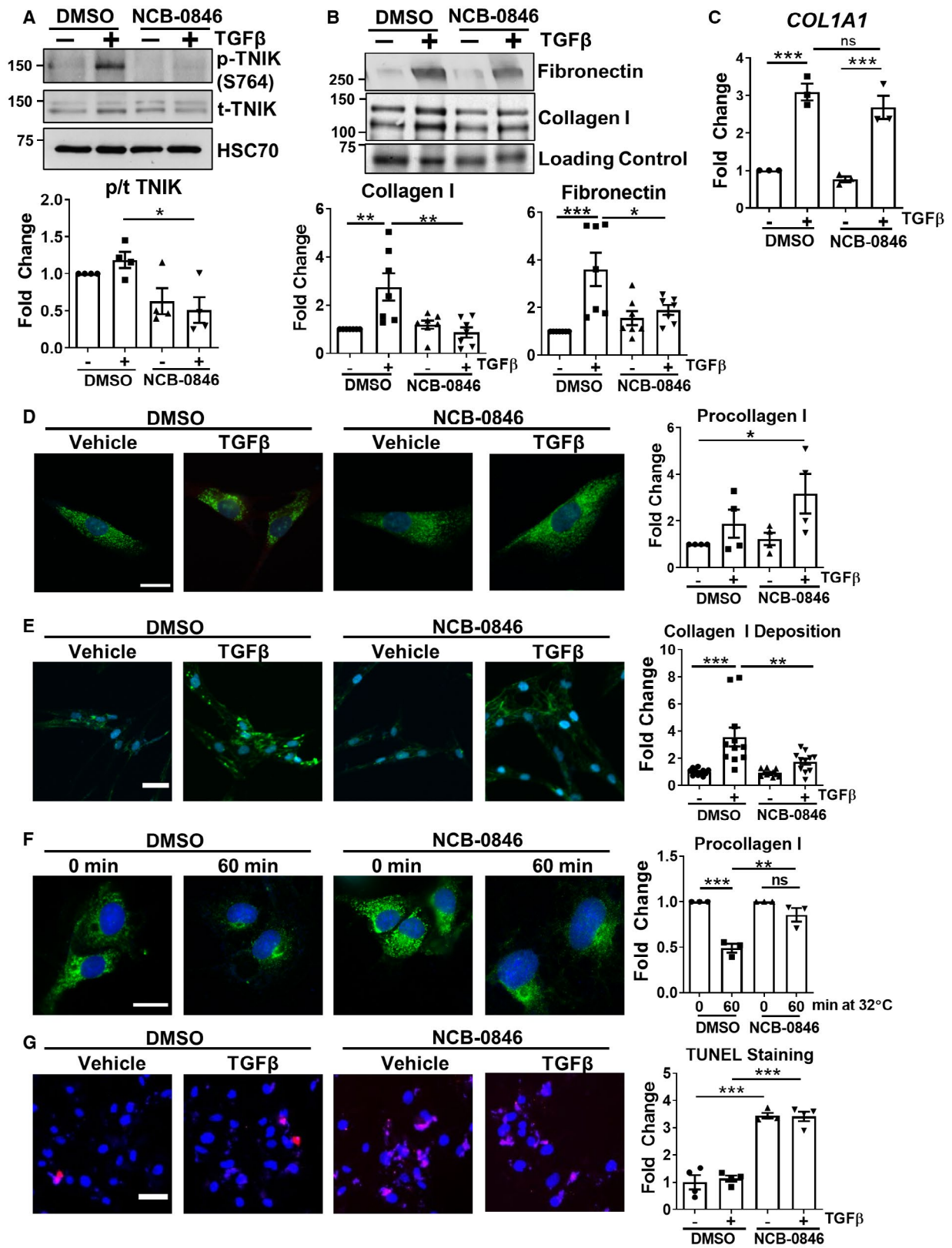
FIG. 3. TNIK kinase activity is critical for procollagen I secretion. (A-E) hHSCs were treated with TGFβ (2 ng/mL) in the presence of NCB-0846 (0.1 μM) or DMSO as a vehicle control. (A) Whole-cell lysates or (B) conditioned media were harvested and analyzed by immunoblotting for intracellular p-TNIK, total TNIK, collagen I, and fibronectin (A, n = 4) or extracellular collagen I and fibronectin (B, n = 7). (C) mRNA was harvested and expression of *COL1A1* was analyzed by qPCR (n = 3). (D,E) Treated hHSCs were fixed, (D) permeabilized, or (E) not permeabilized before staining for collagen I (green) and the nucleus (DAPI, blue) (D scale bar, 20 μm; n = 4; E scale bar, 50 μm; n = 11). (F) mGFP-Col1α1 cells were ascorbate starved and incubated at 40°C in the presence of NCB-0846 or DMSO for 3 hours. Cells were shifted to 32°C in the presence of ascorbate for 0 or 60 minutes, fixed, stained for DAPI, and imaged at magnification ×10 using an AxioObserver scope with six images taken per well (scale bar, 20 μm; n = 3). (G) hHSCs were treated with TGFβ (or vehicle) in the presence of NCB-0846 or DMSO for 48 hours. Cells were fixed and stained with DAPI and Cell Death Detection Kit (Roche) to detect dying cells (DAPI, blue; TUNEL, red). Images were taken at magnification ×10 using an AxioObserver 5 microscope (scale bar, 50 μm; six images per well) and quantified using ImageJ (n = 4). *$P < 0.05$, **$P < 0.01$, ***$P < 0.001$, as calculated by one-way ANOVA followed by Tukey post hoc test. Bars in panels A-G represent mean ± SEM. Abbreviations: min, minutes; ns, not significant; t-TNIK, total TNIK.

subsequently investigated whether disrupted procollagen I trafficking impaired HSC viability by using a TUNEL assay. NCB-0846 treatment (48 hours) increased the percentage of TUNEL-positive HSCs with or without TGFβ treatment (Fig. 3G). Taken together, these results suggest that TNIK kinase activity is required for normal procollagen trafficking and that loss of TNIK kinase activity by NCB-0846 disrupts procollagen I secretion and increases HSC death.

TNIK IS UP-REGULATED IN HUMAN AND MURINE LIVER FIBROSIS AND IN ACTIVATED HSCS

TNIK is involved in neuronal organization and colorectal cancer progression, but the roles of TNIK in the liver and fibrosis are unclear. This prompted us to investigate whether TNIK was involved in the development of liver fibrosis and whether targeting TNIK could limit fibrogenesis. We compared *TNIK* gene expression between healthy and cirrhotic human livers by using a publicly available database and found significant *TNIK* elevation in cirrhotic livers (Fig. 4A).[29] Furthermore, TNIK protein levels increased in primary hHSCs in response to TGFβ (Fig. 4B). To determine if TNIK was similarly regulated in a murine model of fibrosis, we immunoblotted for total TNIK and phosphorylated TNIK (p-TNIK) (S735 in mice) in whole-liver lysates harvested from mice following CCl$_4$ injection (twice weekly for 4 weeks). Both total TNIK and p-TNIK increased in CCl$_4$-treated livers compared to controls (Fig. 4C). These data combined with the role of TNIK in procollagen I trafficking and matrix deposition *in vitro* suggest that targeting TNIK could limit fibrogenesis *in vivo*.

TNIK INHIBITION BY THE SMALL-MOLECULE COMPOUND NCB-0846 REDUCES MURINE LIVER FIBROSIS

To determine if TNIK kinase activity was critical for liver fibrogenesis, age- and sex-matched C57BL/6J mice received intraperitoneal injections of CCl$_4$ (0.5 μL/mg, 0.08 mL/mouse) or olive oil twice weekly for 4 weeks to induce fibrogenesis while simultaneously receiving 10 mg/kg NCB-0846 or a vehicle control 5 times weekly (Fig. 5A). NCB-0846 effectively reduced p-TNIK (S735) in NCB-0846-treated livers without impacting total *Tnik* mRNA expression (Fig. 5B,C). Mice receiving CCl$_4$ in combination with NCB-0846 displayed limited fibrosis compared to CCl$_4$ alone, as shown by sirius red staining (Fig. 6A) and measurement of hydroxyproline content (Fig. 6B). qPCR analysis of whole-liver mRNA revealed that CCl$_4$ increased *Col1a1*, fibronectin 1 (*Fn1*), and platelet-derived growth factor receptor beta (*Pdgfrb*) expression, but this effect was lost in mice receiving CCl$_4$+NCB-0846 (Fig. 6C). This was similarly observed for fibronectin and collagen I protein levels (Fig. 6D). This differs from *in vitro* data where procollagen I expression was unchanged in response to NCB-0846 treatment. We predict this difference is due to long-term effects of NCB-0846 treatment on matrix secretion, as similar *in vitro* and *in vivo* phenotypes were observed where disruption of procollagen I trafficking machinery promotes procollagen I retention *in vitro* but reduces procollagen I expression in long-term *in vivo* models.[13,30] Finally, IHC revealed that NCB-0846 had no effect on CCl$_4$-induced αSMA or TUNEL staining (Fig. 6E,F). While differing from *in vitro* data where NCB-0846 increased
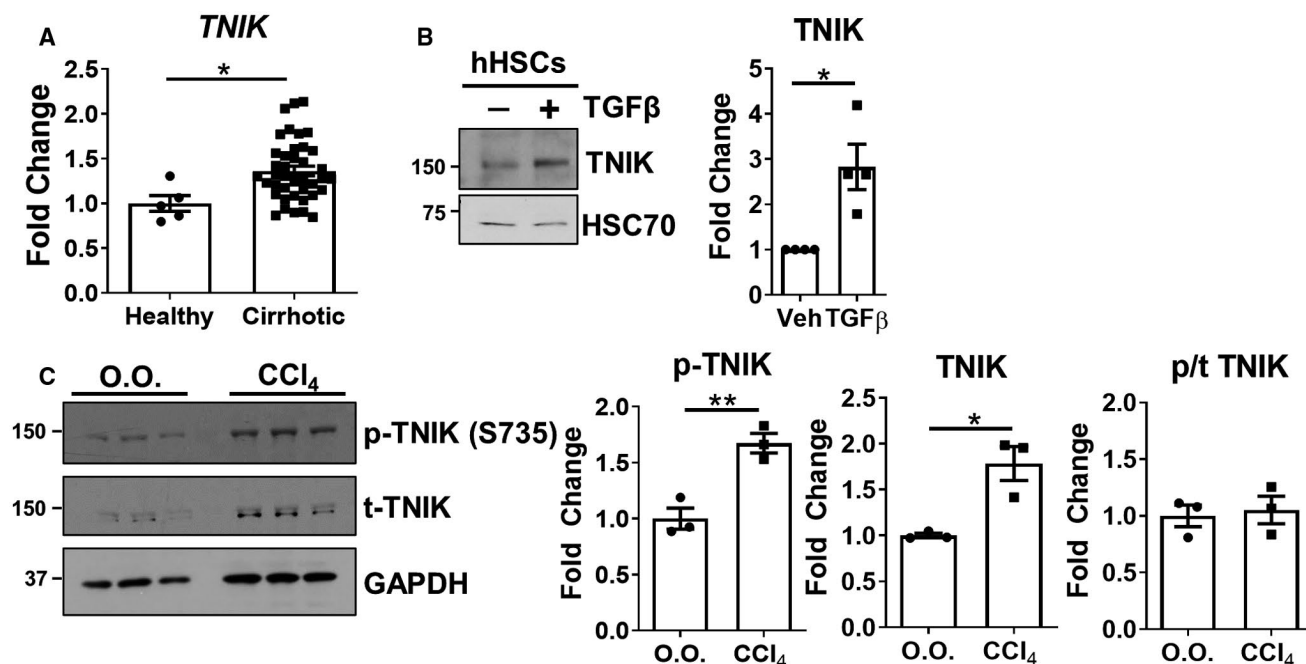
FIG. 4. TNIK levels positively correlate with fibrosis and HSC activation. (A) TNIK expression is increased in livers of patients with cirrhosis compared to noncirrhotic controls (dataset GSE25097, deposited in GEO DataSets). (B) hHSCs were treated with TGFβ (2 ng/mL) for 24 hours, lysed, and analyzed by immunoblotting (n = 4 biological replicates). (C) Mice were injected with CCl_4 (0.5 μL/mg, 0.08 mL/mouse) or olive oil twice a week for 4 weeks, after which whole livers were homogenized and analyzed by immunoblotting (n = 3 mice/condition). *$P < 0.05$, **$P < 0.01$, ***$P < 0.001$, as determined using a paired Student t test. Bars in panels A-C represent mean ± SEM. Abbreviations: GAPDH, glyceraldehyde 3-phosphate dehydrogenase; O.O., olive oil; Veh, vehicle.
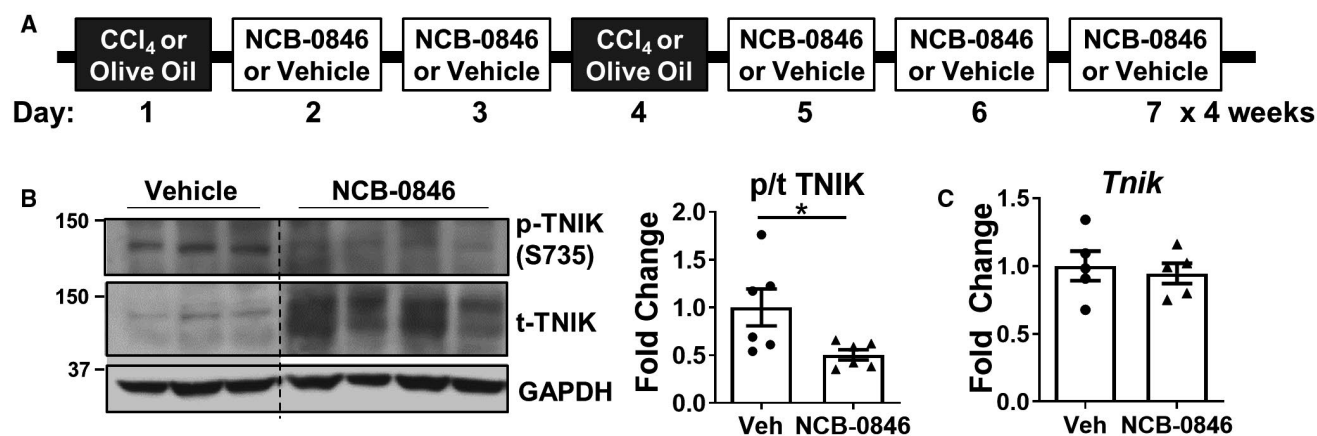

FIG. 5. NCB-0846 injection inhibits TNIK phosphorylation *in vivo*. (A) Fibrosis was induced in age- and sex-matched mice with two weekly intraperitoneal injections of CCl_4 (0.5 μL/mg, 0.08 mL/mouse) or olive oil as a vehicle. The TNIK kinase inhibitor NCB-0846 was injected 5 days/week intraperitoneally (10 mg/kg, 0.03 mL/mouse; vehicle, 70% PEG-300, 15% DMSO, 15% ddH20). After 4 weeks, mice were sacrificed and livers harvested (n = 6-9 mice/group). (B) Whole livers were analyzed by immunoblotting for t-TNIK, p-TNIK (S735), and GAPDH (loading control) (n = 6). *$P < 0.05$, as determined by a paired Student t test. (C) mRNA was harvested from whole liver of mice treated with vehicle or NCB-0846 for 4 weeks (n = 5). Bars in panel B represent mean ± SEM. Abbreviations: GAPDH, glyceraldehyde 3-phosphate dehydrogenase; PEG-300, polyethylene glycol 300; Veh, vehicle.

TUNEL staining, our *in vivo* results do not rule out that NCB-0846 may induce apoptosis of high collagen I-producing HSCs early during fibrosis development, thus contributing to reduced fibrogenesis. Together, these data show that inhibition of TNIK kinase activity impairs fibrogenesis in mice.
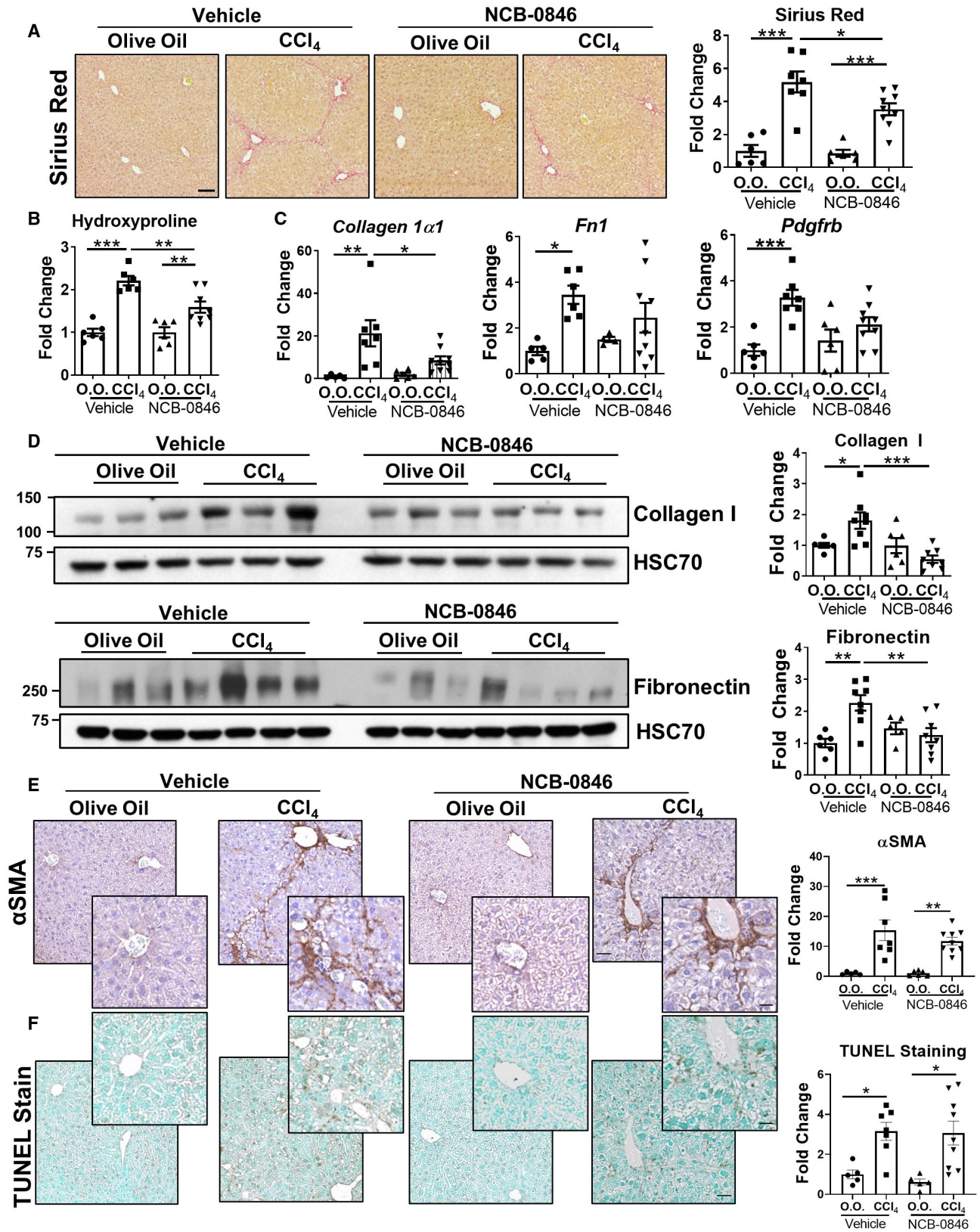
FIG. 6. Inhibition of TNIK kinase activity reduces fibrogenesis *in vivo*. (A) Paraffin-embedded tissues were stained for sirius red to analyze collagen I/III deposition. Five images per tissue were taken at magnification ×10 and analyzed using ImageJ (n = 6-9 mice/group; scale bar, 50 μm). (B) Hydroxyproline analysis was performed to analyze collagen I/III content (n = 6-9 mice/group). (C) mRNA was harvested from whole-liver tissue and analyzed by qPCR for *Col1a1*, *Fn1*, and *Pdgfrb* (n = 6-9 mice/group). (D) Whole-liver tissue was lysed for immunoblotting and analyzed for Col1α1 and fibronectin. HSC70 served as a loading control (n = 6-9 mice/group). (E,F) Paraffin-embedded liver sections were stained for αSMA and TUNEL to analyze HSC activation, and cell death, respectively. Five images per tissue section were taken at magnification ×10 and analyzed using ImageJ. Representative images are shown (n = 6-9 mice/group; scale bar, 50 μm for images, 25 μm for inset). *$P < 0.05$, **$P < 0.01$, ***$P < 0.001$, as determined by one-way ANOVA followed by Tukey post hoc tests for A-F. Bars in panels A-F represent mean ± SEM. Abbreviations: O.O., olive oil; *Pdgfrb*, platelet-derived growth factor receptor beta.

Discussion

Procollagen I secretion and deposition in response to liver injury drives the progression of liver fibrosis; however, there is a lack of effective therapeutics that target this process. The majority of studies targeting collagen I focused on disrupting existing scar tissue, but efforts to date have been ineffective in the clinic. Recent focus has been placed on targeting procollagen I before its release from fibrogenic HSCs by targeting intracellular processing and trafficking of procollagen I. Disrupting procollagen I exit from the ER leads to cellular and ER stress, induction of the unfolded protein response, and HSC apoptosis, which is favorable for fibrosis resolution.[6] While progress is being made targeting proteins involved in procollagen I folding, much of the procollagen I trafficking pathway after ER exit remains unclear and could serve as an antifibrotic target.[31] The goal of our study was to identify proteins involved in procollagen I processing and trafficking that could be targeted *in vivo* to limit fibrogenesis. Our siRNA screen revealed seven targets that increased procollagen I retention *in vitro* that had no known role in procollagen I regulation, including TNIK. TNIK expression and phosphorylation increased in cirrhotic livers and activated HSCs, and inhibition of TNIK kinase activity disrupted procollagen I secretion *in vitro*. Finally, TNIK kinase inhibition reduced CCl$_4$-induced fibrogenesis *in vivo*, highlighting a critical and targetable role for TNIK in hepatic fibrosis (Fig. 7). While increased TUNEL staining in HSCs was not observed following 4 weeks of CCl$_4$ injection, this does not discount the possibility that NCB-0846 induced apoptosis in active collagen I-producing mHSCs earlier in the fibrosis model that would be missed in the current analysis. Furthermore, single-cell RNA sequencing previously identified subpopulations of HSCs that arise during chronic CCl$_4$ treatment. HSC subpopulations could be differentially impacted by long-term TNIK inhibition in our model as we observed decreased procollagen I and fibronectin expression while αSMA was unchanged.[32] Together, our data revealed a crucial fibrogenic role for TNIK in HSCs.

Our siRNA screen to identify proteins critical for procollagen I secretion revealed potential roles for proteins that serve a wide breadth of cellular functions. Within this group were three kinases (TNIK, rho-associated protein kinase 1 [ROCK1], and p21 activated kinase 1 [PAK1]), a guanine nucleotide exchange factor (VAV2), a guanosine triphosphatase (RAB5A), as well as other scaffolding and trafficking proteins (syntaxin 1 [SNX1], intersectin 1 [ITSN1], disabled homolog 2 [DAB2], COPA). The identification of COPA fit well with previous studies as retrograde trafficking of ER Golgi intermediate compartments (ERGICs), a process involving COPA, is critical for formation of procollagen I-containing COPII vesicles.[21] The other identified proteins play various roles in membrane trafficking, including both exocytic and endocytic trafficking (DAB2, RAB5, ITSN1). One potential role for endocytic proteins in procollagen I secretion is enlargement of procollagen I-containing vesicles, similar to the function of ERGIC membranes at ER exit sites.[21] Additionally, disruption of endocytosis could alter the homeostatic balance between exocytosis and endocytosis. A recent study suggested that collagen I can be taken up by cells through endocytosis and recycled back to the plasma membrane for reassembly and secretion.[33] Furthermore, mass spectrometry aimed at identifying proteins involved in procollagen I reuptake found a potential role for DAB2, a top hit in our screen.[33] Continued study of DAB2 and the other endocytic proteins identified by our siRNA screen would provide additional insight into the fibrogenic process and procollagen I biology.
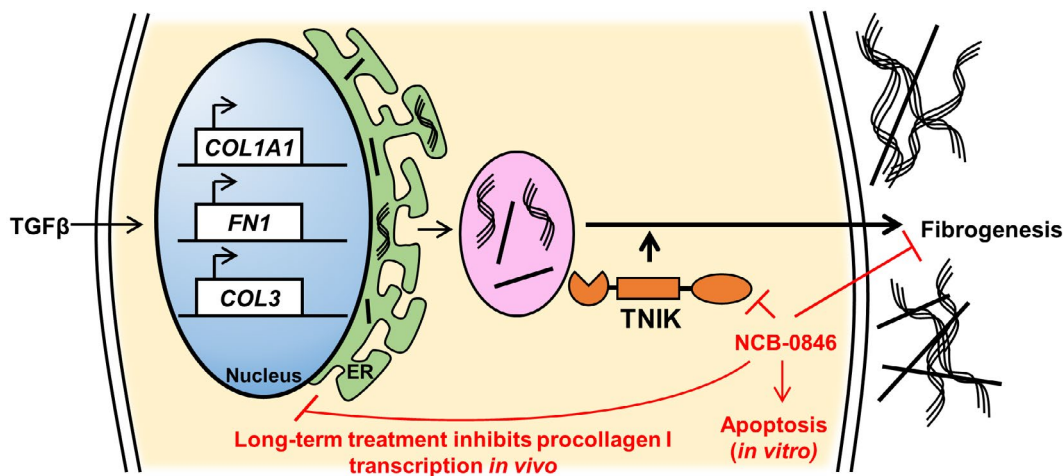
FIG. 7. TNIK kinase activity is critical for procollagen I trafficking and fibrogenesis. Activation of HSCs by factors such as TGFβ leads to expression of extracellular matrix genes, such as *COL1A1* and *FN1*. These transcripts are cotranslationally translocated into the ER. Following exit from the ER, secretory vesicles containing procollagen I and fibronectin are trafficked and secreted in a TNIK-dependent manner to drive fibrogenesis. Inhibition of TNIK kinase activity through NCB-0846 disrupts procollagen I trafficking *in vitro* and fibrogenesis *in vivo*, while long-term TNIK inhibition limits procollagen I expression. Abbreviation: ER, endoplasmic reticulum.

Procollagen I folding and trafficking requires numerous steps and specific chaperones/binding proteins, including prolyl hydroxylase (P4H) subunits A1, A2, and B, in addition to the collagen-specific chaperone HSP47.[6] Folded procollagen I is recruited to TANGO1-containing ER exit sites, but following ER exit, the mechanisms and regulation of procollagen I trafficking remain unclear. We have observed that when procollagen I trafficking is disrupted, as with TNIK inhibition or the loss of TANGO1, procollagen I accumulation is observed by immunofluorescence, often as large globular structures.[7,12,34] With TANGO1 deletion, these procollagen I-positive structures colocalize with ER markers, but with TNIK inhibition, procollagen I does not colocalize with ER or Golgi markers.[7] Furthermore, we observed that TNIK regulated fibronectin and collagen III secretion, suggesting a wider role for TNIK in protein secretion. This raises the following three outstanding questions: 1) Where and by what mechanism(s) does TNIK regulate procollagen I trafficking? 2) Why is fibronectin similarly dysregulated? and 3) What happens to retained procollagen I? We will discuss these questions in detail to gain insight into the possible roles of TNIK in fibrogenic HSCs.

TNIK was initially discovered in neurons, playing a critical role in organization of the postsynaptic density (PSD).[23,35] Within the PSD, TNIK interacted with receptors, including glutamate receptor subunit 1 (GluR1) and endosomal vesicles.[24] TNIK binding to and subsequent phosphorylation of GluR1 was essential for recycling of GluR1-containing vesicles to the plasma membrane.[24] This role was regulated by Rap2a, a small GTPase that regulates endosomal trafficking.[24] TNIK binding to Rap2a at the PSD induced TNIK autophosphorylation and subsequent cytoskeletal rearrangement.[36] Rap2 activation also promoted redistribution of TNIK of SNX6-positive post-Golgi endosomal vesicles.[24] This provides precedence for TNIK localization at post-Golgi vesicles where it might regulate procollagen I trafficking in HSCs. Further analysis of the functional role of TNIK and its regulators (e.g., Rap2 and GluR1) is needed to understand the mechanisms of TNIK-mediated matrix secretion.

A potential role for TNIK involvement in the trafficking of matrix proteins lies in the ability of TNIK to organize the actin cytoskeleton. In neurons, TNIK kinase activity regulated cytoskeleton organization through both c-Jun N-terminal kinase signaling and Rap2.[23,37] Mass spectrometry further revealed other cytoskeletal-associated proteins as putative TNIK substrates, including actin remodeling proteins formin-like 2 (FMNL2) and mammalian enabled

(Mena); however, the consequence of this phosphorylation is unknown.[38] TNIK regulation of the actin cytoskeleton could facilitate trafficking of procollagen I-containing vesicles or fusion/enlargement of trafficking vesicles. TNIK also influences mitogen-activated protein kinase (MAPK) signaling cascades and enters the nucleus to promote Wnt signaling and drive colon cancer progression.[25,26,39] Given the diverse roles of TNIK in neurons and cancer, understanding whether TNIK regulates fibrogenesis through different mechanisms is critical for targeting TNIK as an antifibrotic strategy.

While our focus has been primarily on procollagen I, fibronectin and collagen III secretion were also disrupted by TNIK inhibition or loss in HSCs. Fibronectin secretion by HSCs is critical for collagen I/III to be incorporated into the matrix, thus playing an important role in liver fibrosis.[40] Similar to procollagen I, fibronectin is folded in the ER and trafficked through the Golgi, although exit of fibronectin from the ER does not require TANGO1.[7] Separate studies showed fibronectin and procollagen I co-immunoprecipitate intracellularly and that fibronectin trafficking from the Golgi to the plasma membrane involves late endosomes and lysosomes.[41,42] This supports a potential post-Golgi role for TNIK in fibronectin and procollagen I/III trafficking. Future studies of the mechanisms of TNIK function in regulating cytoskeletal and endosomal networks in HSCs would provide insight into the trafficking mechanisms of fibronectin, procollagen I/III, and potentially other secretory cargos.

Additional questions remain regarding the fate of retained procollagen I following TNIK inhibition/deletion. We observed procollagen I retention by immunofluorescence, but immunoblotting did not reveal an appreciable increase in intracellular procollagen I. We propose two possible explanations, degradation and insolubility. Degradation is a possible explanation because 10%-30% of procollagen translocated into the ER is degraded, with this portion elevated when procollagen I is mutated. This degradation occurs through the following three distinct processes: autophagy/ERphagy, ubiquitin-mediated proteasomal degradation, and lysosomal degradation.[34,43-48] Procollagen I retention in response to TNIK loss or inhibition may be driving these degradative processes in an effort to relieve cellular stress caused by procollagen I accumulation. Insolubility of retained procollagen I may also be responsible for why we observe increased procollagen I by immunofluorescence but not immunoblotting. Deletion of HSP47 causes procollagen I to accumulate into detergent-insoluble aggregates, which may be occurring similarly following TNIK inhibition/deletion in our assays.[34] We anticipate that degradation, insolubility, or a combination of both is occurring in LX-2 cells lacking TNIK or treated with NCB-0846.

A major gap in our understanding of TNIK in HSCs and fibrogenesis is that few studies have interrogated the importance of TNIK in fibroblasts or mesodermal cell lineages from which HSCs are derived. The majority of studies looking at TNIK and Wnt signaling were conducted in epithelial cells, while studies interrogating the role of TNIK in scaffolding and actin organization have focused on neuronal cells. It is critical to elucidate the processes TNIK is required for in HSCs and other fibroblasts to better understand how TNIK promotes fibrogenesis. A clue to how TNIK may influence HSCs is axonal signaling. Analysis of publicly available databases reveals that one of the up-regulated canonical pathways in activated HSCs is the axonal guidance pathway.[49,50] This includes neuropilin, Wnt-associated genes, matrix metalloproteinases, and actin regulatory genes (myosin light chain 4 [*Myl4*], *Myl10*, actin-binding lim protein 2 (*Ablim2*).[49,50] Thus, in addition to regulating procollagen I trafficking, TNIK could serve additional cell-specific roles in fibrogenesis and HSCs that merit further study.

In summary, we tested and validated the efficacy of a novel *in vitro* screen to identify potential antifibrotic targets with *in vivo* efficacy. We identified seven genes with no previously known role in procollagen I trafficking. Deeper investigation revealed a crucial role for TNIK in procollagen I trafficking that could be pharmacologically targeted *in vitro* and *in vivo* to limit fibrogenesis. Future experiments will further elucidate the mechanistic role of TNIK in procollagen I and other fibrogenic trafficking, investigate additional functions of TNIK in HSCs and other cell types, as well as elucidate the role of other mediators of procollagen I trafficking identified in our screen and their potential role in hepatic fibrosis.

REFERENCES

1) **Berumen J**, **Baglieri J**, Kisseleva T, Mekeel K, Mekeel K. Liver fibrosis: pathophysiology and clinical implications. Wiley Interdiscip Rev Syst Biol Med 2021;13:e1499.

2) **Iwaisako K**, **Jiang C**, Zhang M, Cong M, Moore-Morris TJ, Park TJ, et al. Origin of myofibroblasts in the fibrotic liver in mice. Proc Natl Acad Sci U S A 2014;111:E3297-E3305.

3) Ezhilarasan D, Sokal E, Najimi M. Hepatic fibrosis: it is time to go with hepatic stellate cell-specific therapeutic targets. Hepatobiliary Pancreat Dis Int 2018;17:192-197.

4) Higashi T, Friedman SL, Hoshida Y. Hepatic stellate cells as key target in liver fibrosis. Adv Drug Deliv Rev 2017;121:27-42.

5) Maiers JL, Malhi H. Endoplasmic reticulum stress in metabolic liver diseases and hepatic fibrosis. Semin Liver Dis 2019;39:235-248.

6) Ishikawa Y, Bachinger HP. A molecular ensemble in the rER for procollagen maturation. Biochim Biophys Acta 2013;1833:2479-2491.

7) Maiers JL, Kostallari E, Mushref M, deAssuncao TM, Li H, Jalan-Sakrikar N, et al. The unfolded protein response mediates fibrogenesis and collagen I secretion through regulating TANGO1 in mice. Hepatology 2017;65:983-998.

8) Nagata K, Saga S, Yamada KM. Characterization of a novel transformation-sensitive heat-shock protein (HSP47) that binds to collagen. Biochem Biophys Res Commun 1988;153:428-434.

9) Lamande SR, Bateman JF. Procollagen folding and assembly: the role of endoplasmic reticulum enzymes and molecular chaperones. Semin Cell Dev Biol 1999;10:455-464.

10) Malhotra V, Erlmann P. The pathway of collagen secretion. Annu Rev Cell Dev Biol 2015;31:109-124.

11) Saito K, Chen M, Bard F, Chen S, Zhou H, Woodley D, et al. TANGO1 facilitates cargo loading at endoplasmic reticulum exit sites. Cell 2009;136:891-902.

12) Ito S, Ogawa K, Takeuchi K, Takagi M, Yoshida M, Hirokawa T, et al. A small-molecule compound inhibits a collagen-specific molecular chaperone and could represent a potential remedy for fibrosis. J Biol Chem 2017;292:20076-20085.

13) **Sato Y**, **Murase K**, Kato J, Kobune M, **Sato T**, Kawano Y, et al. Resolution of liver cirrhosis using vitamin A-coupled liposomes to deliver siRNA against a collagen-specific chaperone. Nat Biotechnol 2008;26:431-442.

14) **Doench JG**, **Fusi N**, Sullender M, Hegde M, Vaimberg EW, Donovan KF, et al. Optimized sgRNA design to maximize activity and minimize off-target effects of CRISPR-Cas9. Nat Biotechnol 2016;34:184-191.

15) **Sanjana NE**, **Shalem O**, Zhang F. Improved vectors and genome-wide libraries for CRISPR screening. Nat Methods 2014;11:783-784.

16) **Xue F**, **Lu J**, **Buchl SC**, Sun L, Shah VH, Malhi H, et al. Coordinated signaling of activating transcription factor 6alpha and inositol requiring enzyme 1alpha regulates hepatic stellate cell-mediated fibrogenesis in mice. Am J Physiol Gastrointest Liver Physiol 2021;320:G864-G879.

17) **Shao Y**, **Wichern E**, Childress PJ, Adaway M, Misra J, Klunk A, et al. Loss of Nmp4 optimizes osteogenic metabolism and secretion to enhance bone quality. Am J Physiol Endocrinol Metab 2019;316:E749-E772.

18) McCaughey J, Stevenson NL, Cross S, Stephens DJ. ER-to-golgi trafficking of procollagen in the absence of large carriers. J Cell Biol 2019;218:929-948.

19) Subramanian A, Capalbo A, Iyengar NR, Rizzo R, di Campli A, Di Martino R, et al. Auto-regulation of secretory flux by sensing and responding to the folded cargo protein load in the endoplasmic reticulum. Cell 2019;176:1461-1476.e1423.

20) Hu Y, Hu D, Yu H, Xu W, Fu R. Hypoxiainducible factor 1alpha and ROCK1 regulate proliferation and collagen synthesis in hepatic stellate cells under hypoxia. Mol Med Rep 2018;18:3997-4003.

21) **Santos AJ**, **Raote I**, Scarpa M, Brouwers N, Malhotra V. TANGO1 recruits ERGIC membranes to the endoplasmic reticulum for procollagen export. Elife 2015;4.e10982.

22) Stephens DJ, Pepperkok R. Imaging of procollagen transport reveals COPI-dependent cargo sorting during ER-to-Golgi transport in mammalian cells. J Cell Sci 2002;115:1149-1160.

23) Fu CA, Shen M, Huang BC, Lasaga J, Payan DG, Luo Y. TNIK, a novel member of the germinal center kinase family that activates the c-Jun N-terminal kinase pathway and regulates the cytoskeleton. J Biol Chem 1999;274:30729-30737.

24) Hussain NK, Hsin H, Huganir RL, Sheng M. MINK and TNIK differentially act on Rap2-mediated signal transduction to regulate neuronal structure and AMPA receptor function. J Neurosci 2010;30:14786-14794.

25) **Mahmoudi T**, **Li VSW**, Ng SS, Taouatas N, Vries RGJ, Mohammed S, et al. The kinase TNIK is an essential activator of Wnt target genes. EMBO J 2009;28:3329-3340.

26) Shitashige M, Satow R, Jigami T, Aoki K, Honda K, Shibata T, et al. Traf2- and Nck-interacting kinase is essential for Wnt signaling and colorectal cancer growth. Cancer Res 2010;70:5024-5033.

27) Wang Q, Charych EI, Pulito VL, Lee JB, Graziane NM, Crozier RA, et al. The psychiatric disease risk factors DISC1 and TNIK interact to regulate synapse composition and function. Mol Psychiatry 2011;16:1006-1023.

28) Masuda M, Uno Y, Ohbayashi N, Ohata H, Mimata A, Kukimoto-Niino M, et al. TNIK inhibition abrogates colorectal cancer stemness. Nat Commun 2016;7:12586.

29) Tung E-K, Mak C-M, Fatima S, Lo R-L, Zhao H, Zhang C, et al. Clinicopathological and prognostic significance of serum and tissue Dickkopf-1 levels in human hepatocellular carcinoma. Liver Int 2011;31:1494-1504.

30) Kawasaki K, Ushioda R, Ito S, Ikeda K, Masago Y, Nagata K. Deletion of the collagen-specific molecular chaperone Hsp47 causes endoplasmic reticulum stress-mediated apoptosis of hepatic stellate cells. J Biol Chem 2015;290:3639-3646.

31) Miyamura T, Sakamoto N, Kakugawa T, Taniguchi H, Akiyama Y, Okuno D, et al. Small molecule inhibitor of HSP47 prevents profibrotic mechanisms of fibroblasts in vitro. Biochem Biophys Res Commun 2020;530:561-565.

32) Krenkel O, Hundertmark J, Ritz TP, Weiskirchen R, Tacke F. Single cell RNA sequencing identifies subsets of hepatic stellate cells and myofibroblasts in liver fibrosis. Cells 2019;8:503.

33) Chang J, Pickard A, Garva R, Lu Y, Gullberg D, Kadler KE. The endosome is a master regulator of plasma membrane collagen fibril assembly. bioRxiv 2021; https://doi.org/10.1101/2021.03.25.436925.

34) Ishida Y, Yamamoto A, Kitamura A, Lamandé SR, Yoshimori T, Bateman JF, et al. Autophagic elimination of misfolded procollagen aggregates in the endoplasmic reticulum as a means of cell protection. Mol Biol Cell 2009;20:2744-2754.

35) Burette AC, Phend KD, Burette S, Lin Q, Liang M, Foltz G, et al. Organization of TNIK in dendritic spines. J Comp Neurol 2015;523:1913-1924.

36) **Uechi Y**, **Bayarjargal M**, Umikawa M, Oshiro M, Takei K, Yamashiro Y, et al. Rap2 function requires palmitoylation and

recycling endosome localization. Biochem Biophys Res Commun 2009;378:732-737.

37) Taira K, Umikawa M, Takei K, Myagmar B-E, Shinzato M, Machida N, et al. The Traf2- and Nck-interacting kinase as a putative effector of Rap2 to regulate actin cytoskeleton. J Biol Chem 2004;279:49488-49496.

38) Wang Q, Amato SP, Rubitski DM, Hayward MM, Kormos BL, Verhoest PR, et al. Identification of phosphorylation consensus sequences and endogenous neuronal substrates of the psychiatric risk kinase TNIK. J Pharmacol Exp Ther 2016;356:410-423.

39) **Larhammar M**, **Huntwork-Rodriguez S**, Rudhard Y, Sengupta-Ghosh A, Lewcock JW. The Ste20 family kinases MAP4K4, MINK1, and TNIK converge to regulate stress-induced JNK signaling in neurons. J Neurosci 2017;37:11074-11084.

40) Sottile J, Shi F, Rublyevska I, Chiang HY, Lust J, Chandler J. Fibronectin-dependent collagen I deposition modulates the cell response to fibronectin. Am J Physiol Cell Physiol 2007;293:C1934-C1946.

41) **Armstrong HK**, **Gillis JL**, Johnson IRD, Nassar ZD, Moldovan M, Levrier C, et al. Dysregulated fibronectin trafficking by Hsp90 inhibition restricts prostate cancer cell invasion. Sci Rep 2018;8:2090.

42) DiChiara AS, Taylor RJ, Wong MY, Doan ND, Rosario AM, Shoulders MD. Mapping and exploring the collagen-I proteostasis network. ACS Chem Biol 2016;11:1408-1421.

43) **Forrester A**, **De Leonibus C**, **Grumati P**, **Fasana E**, Piemontese M, Staiano L, et al. A selective ER-phagy exerts procollagen quality control via a calnexin-FAM134B complex. EMBO J 2019;38:e99847.

44) Fregno I, Fasana E, Solda T, Galli C, Molinari M. N-glycan processing selects ERAD-resistant misfolded proteins for ER-to-lysosome-associated degradation. EMBO J 2021;40:e107240.

45) **Kim SI**, **Na HJ**, Ding Y, Wang Z, Lee SJ, Choi ME. Autophagy promotes intracellular degradation of type I collagen induced by transforming growth factor (TGF)-beta1. J Biol Chem 2012;287:11677-11688.

46) Nabavi N, Pustylnik S, Harrison RE. Rab GTPase mediated procollagen trafficking in ascorbic acid stimulated osteoblasts. PLoS One 2012;7:e46265.

47) Nabavi N, Urukova Y, Cardelli M, Aubin JE, Harrison RE. Lysosome dispersion in osteoblasts accommodates enhanced collagen production during differentiation. J Biol Chem 2008;283:19678-19690.

48) Ko MK, Kay EP. PDI-mediated ER retention and proteasomal degradation of procollagen I in corneal endothelial cells. Exp Cell Res 2004;295:25-35.

49) **Drinane MC**, **Yaqoob U**, **Yu H**, **Luo F**, Greuter T, Arab JP, et al. Synectin promotes fibrogenesis by regulating PDGFR isoforms through distinct mechanisms. JCI Insight 2017;2:e92821.

50) Martin-Mateos R, De Assuncao TM, Arab JP, Jalan-Sakrikar N, Yaqoob U, Greuter T, et al. Enhancer of zeste homologue 2 inhibition attenuates TGF-beta dependent hepatic stellate cell activation and liver fibrosis. Cell Mol Gastroenterol Hepatol 2019;7:197-209.

Author names in bold designate shared co-first authorship.

Supporting Information

Additional Supporting Information may be found at onlinelibrary.wiley.com/doi/10.1002/hep4.1835/suppinfo.